The Journal of Experimental Biology 212, 1593-1603
Published by The Company of Biologists 2009
doi:10.1242/jeb.026708

Review

NhaA crystal structure: functional–structural insights

Etana Padan*, Lena Kozachkov, Katia Herz and Abraham Rimon

Department of Biological Chemistry, Alexander Silberman Institute of Life Sciences, The Hebrew University of Jerusalem, 91904 Jerusalem, Israel

*Author for correspondence (e-mail: etana@vms.huji.ac.il)

Accepted 19 November 2008

Summary

Na^+/H^+ antiporters are integral membrane proteins that exchange Na^+ for H^+ across the cytoplasmic membrane and many intracellular membranes. They are essential for Na^+, pH and volume homeostasis, which are crucial processes for cell viability. Accordingly, antiporters are important drug targets in humans and underlie salt-resistance in plants. Many Na^+/H^+ antiporters are tightly regulated by pH. *Escherichia coli* NhaA Na^+/H^+ antiporter, a prototype pH-regulated antiporter, exchanges 2 H^+ for 1 Na^+ (or Li^+). The NhaA crystal structure has provided insights into the pH-regulated mechanism of antiporter action and opened up new *in silico* and *in situ* avenues of research. The monomer is the functional unit of NhaA yet the dimer is essential for the stability of the antiporter under extreme stress conditions. Ionizable residues of NhaA that strongly interact electrostatically are organized in a transmembrane fashion in accordance with the functional organization of the cation-binding site, 'pH sensor', the pH transduction pathway and the pH-induced conformational changes. Remarkably, NhaA contains an inverted topology motive of transmembrane segments, which are interrupted by extended mid-membrane chains that have since been found to vary in other ion-transport proteins. This novel structural fold creates a delicately balanced electrostatic environment in the middle of the membrane, which might be essential for ion binding and translocation. Based on the crystal structure of NhaA, a model structure of the human Na^+/H^+ exchanger (NHE1) was constructed, paving the way to a rational drug design.

Key words: NhaA, NHA, NHE, Na^+/H^+ antiporters, active transport, membrane proteins.

Na^+/H^+ antiporters – a major family of integral membrane proteins

Every cell and organelle is separated from its environment by a membrane with a dual function; on the one hand, it is impermeable to solutes and protects the cell or organelle from its environment; on the other hand, embedded in it are integral membrane proteins that are responsible for the communication between the cell and its environment. These proteins are responsible for cell bioenergetics (photosynthesis and respiration), signal transduction and the transport of solutes and ions across the membrane. The genome and the proteome projects reveal that the integral membrane proteins comprise about 30% of each proteome and form about 60% of the targets for human drugs and plant herbicides.

Na^+/H^+ antiporters are a vast family of integral membrane proteins. They play a primary role in regulating the intracellular pH, Na^+ content and volume of all cells. Homeostasis of H^+, Na^+ and volume are crucial for every cell because when the concentration of intracellular Na^+ and H^+ becomes either too high or too low they turn into potent stressors to all cells. The Na^+/H^+ antiporter activity was discovered by Peter Mitchell and colleagues in the early seventies of the last century (West and Mitchell, 1974). Since then, this activity has been found in the cytoplasmic membrane and in many organelle membranes throughout the biological kingdom, from bacteria to higher plants and humans (Padan, 2008).

The genome project has yielded a multiplicity of genes encoding putative Na^+/H^+ antiporters. These were classified as a super family of monovalent cation/proton antiporters (CPA, http://www.tcdb.org/). Two subfamilies, Na^+/H^+ exchanger (NHE) (Orlowski and Grinstein, 2004) and NHA (Brett et al., 2005), have orthologs from bacteria to human. The NHE subfamily includes the nine human NHEs that play critical roles in human heart, kidney and stomach (Malo and Fliegel, 2006; Orlowski and Grinstein, 2004; Slepkov et al., 2007; Wakabayashi et al., 2003). For example, NHE1 has a role in heart hypertrophy and in the damage that occurs during ischemia and reperfusion. In plants, NHE orthologs are used to engineer salt-resistant plants (Apse and Blumwald, 2007; Yamaguchi and Blumwald, 2005). The NHA subfamily has recently been discovered by Rajini Rao, Mark Donowitz and their colleagues (Brett et al., 2005) and is found to be widely spread both in eukaryotes (Battaglino et al., 2008; Day et al., 2008; Fuster, et al., 2008; Pham et al., 2007; Rheault et al., 2007) and prokaryotes (Brett et al., 2005; Padan, 2008). This subfamily includes NhaA of *Escherichia coli*, the subject of this review, and the human NHA1 and NHA2. NHA2 has been suggested to be a candidate gene for essential hypertension (Xiang et al., 2007). We have recently shown that NHE and NHA share a common evolutionary origin and possibly also have a similar structural fold (Brett et al., 2005; Landau et al., 2007).

In spite of their importance and vast distribution, many of the membrane proteins are still an enigma because they are very difficult to study. Unlike the soluble proteins, these proteins are embedded in the membrane and can only be solubilized by detergents. To measure their activity they have to be reconstituted back into a membrane. Furthermore, only recently have the 3-D crystal structures of very few of these proteins been solved. About 40,000 structures of soluble proteins are known whereas only about

150 structures of integral membrane proteins have been determined. Hence, it is still a great challenge to get the crystal structure of an integral membrane protein. NhaA is an educative example for the functional/structural insights gained by the crystal structure of an antiporter.

The family prototype *Escherichia coli* NhaA has been studied most extensively. It is essential for the homeostasis of Na^+ and H^+ in *E. coli* (Padan, 2008; Padan et al., 2005; Padan et al., 2004) and it is also most important in the Na^+ cycle in *Vibrio cholerae* (Herz et al., 2003) and many other bacteria (Padan et al., 2001).

Being involved in the homeostasis of Na^+ and H^+ implies that NhaA must possess certain unique properties; in addition to its capacity to exchange the ions, it must be equipped with 'sensor(s)' to sense the concentrations of Na^+ and/or H^+ in the environment and it must also have the capacity to transduce these environmental signals into a change in activity so that homeostasis is maintained. The response to Na^+ occurs at the transcription level (Padan et al., 2004) whereas the response to H^+ is a function of the protein itself (Padan, 2008).

This review is dedicated to the NhaA protein, focusing on the encounter between the crystal structure of NhaA that we determined at the end of 2005 (Hunte et al., 2005) and the functional data that has been obtained over the years (Padan, 2008).

Paving the way to structural biology of NhaA

The first crucial step forward in the study of the NhaA protein was achieved by constructing a most efficient system for the over-expression and purification of NhaA (Olami et al., 1997). In this system, NhaA fused to six histidines at its C-terminus, is expressed from the regulated, strong *tac* promoter. The His-tagged protein is affinity purified on a Ni-NTA affinity column, in amounts as high as 4–5 $mg\,l^{-1}$ of cells. It can easily be concentrated to 40 $mg\,ml^{-1}$ (Venturi and Padan, 2002).

Most importantly, the purified NhaA is fully active when reconstituted into proteoliposomes and shows all of its unique characteristics that underpin its role in the homeostasis of Na^+ and pH (Padan et al., 2005). Mutants deficient in any of these properties lose resistance to Na^+ and alkaline pH in the presence of Na^+ (Padan et al., 2005; Tzubery et al., 2008). NhaA activity is electrogenic, exchanging $2H^+/1Na^+$ (Taglicht et al., 1993), and has very high turnover rate of $10^5\,min^{-1}$ (Taglicht et al., 1991), NhaA activity is strictly regulated by pH, a property it shares with many other prokaryotic and eukaryotic antiporters (Padan et al., 2004; Taglicht et al., 1991). The activity of NhaA alters by over three-orders of magnitude between pH 6.5 (no activity) and pH 8.5 (maximal activity). Remarkably, NhaA activity is half-maximal at the cytoplasmic pH of 7.6 (Padan et al., 1976).

At acidic pH, NhaA is downregulated and exists in a locked conformation. We believe that this property, together with the high yield of pure and active NhaA, paved the way to the structural biology of NhaA (Screpanti et al., 2006). NhaA crystals that diffract X-rays at 3.45 Å resolution were obtained and allowed us to determine the structure of NhaA (Hunte et al., 2005).

The overall architecture of NhaA

The NhaA molecule is composed of 12 transmembrane segments (TMSs) with N- and C-termini exposed to the cytoplasm (Fig. 1A) (Hunte et al., 2005). The periplasmic face of NhaA is flat and rigid because of structured loops close to the lipid bilayer, including a double-stranded beta sheet. The cytoplasmic face is rough with flexible loops and several helices that protrude into the cytoplasm. A cross-section normal to the membrane shows the presence of cytoplasmic and periplasmic funnels (Fig. 1B) (Hunte et al., 2005). They point to each other but are separated by a hydrophobic barrier. Based on computation, the orifice of the cytoplasmic funnel is potentially accessible to water and hydrated Na^+, Li^+, K^+ and even Ca^{2+}. The funnel then narrows and can only accommodate non-hydrated Na^+ or Li^+ (Fig. 1B) (Hunte et al., 2005).

The 3-D structure of NhaA represents a native conformation

For crystallization, a membrane protein is extracted from the membrane with detergents, which may or may not correctly replace the membrane. The crystal lattice can also modify the protein's native conformation. Nevertheless, reliable procedures for

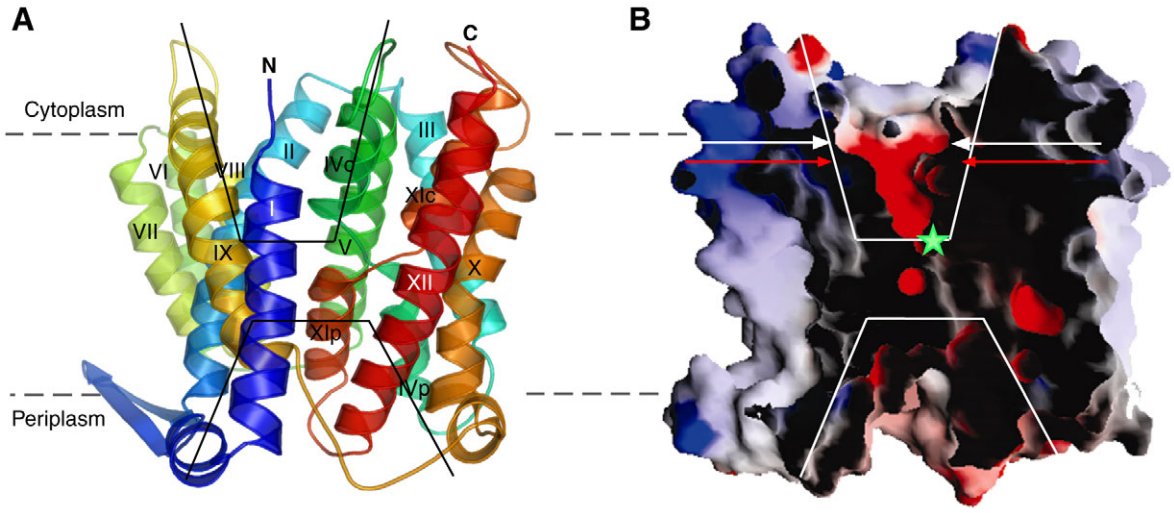

Fig. 1. General architecture of NhaA Na^+/H^+ antiporter. (A) Ribbon representation of the crystal structure of NhaA, viewed parallel to the membrane (broken lines). The 12 transmembrane segments (TMSs) are labeled with roman numerals. **N** and **C** indicate the N- and C-termini, respectively. Cytoplasmic and periplasmic funnels are marked by continuous black lines; c or p denotes helices in the cytoplasmic or periplasmic sides, respectively. (B) Cross-section through the antiporter, normal to the membrane, with the front part removed. The cytoplasmic and periplasmic funnels are marked by white lines. Down to the white arrow, hydrated cations are potentially accessible into the cytoplasmic funnel. Below the red arrow, only non-hydrated Na^+ or Li^+ can potentially enter. The location of D164 is marked by a green star. For further details, see Hunte et al. (Hunte et al., 2005).

determining whether a crystal structure is native are available; NhaA is an example.

One approach is cryo-electron microscopy (cyro-EM) of two-dimensional (2-D) crystals. These crystals are obtained from a membrane-embedded protein, which is therefore suggested to represent a native conformation (Baumeister and Steven, 2000). We have previously obtained very good 2-D crystals of NhaA (Williams, 2000; Williams et al., 1999). Cryo-EM of these crystals provided an electron density map of NhaA. It revealed that NhaA is a dimer in the membrane and that each monomer has 12 TMSs. Although the α-helices were well defined in each NhaA monomer, it has not been possible to assign either helices or loops.

Once the 3-D crystal structure of NhaA had been determined, the helices were assigned and we could use the 2-D map for assessing whether the crystal structure of NhaA is native (Screpanti et al., 2006). We aligned the electron densities from the two techniques and revealed that all helices superimposed well with the EM map; the helix packing of the NhaA monomer in the 3-D crystal structure was identical to that in the 2-D crystal structure (Screpanti et al., 2006). Thus, the NhaA X-ray crystal structure can be reliably assumed to represent a native conformation of the antiporter. Notably, up to now, no such alignment has been done for secondary transporters other than NhaA. We believe that this approach will prove to be an important tool for validating the native conformations of secondary transporters.

Structural information can be obtained by indirect techniques (Guan and Kaback, 2006; Guan and Kaback, 2007; Padan, 2008). Therefore, these techniques are also useful to test whether a crystal structure is native. The most frequently used approaches allow distances within and between membrane proteins to be estimated. These approaches are based on cystein (cys)-replacement in a functional cys-less version of the membrane protein (Guan and Kaback, 2006; Guan and Kaback, 2007; Padan, 2008; Rimon et al., 2002; Tamura et al., 2001). The cys-replacements are chemically modified by thiol-specific probes that enable intervening distances to be estimated by means of pyrene-excimer fluorescence, fluorescence resonance energy transfer (FRET), electron spin resonance (ESR) and thiol cross-linking. The latter is the most user friendly approach, which can easily be used *in situ* on the membrane. The estimated distances are then compared with those in the crystal structure and are used to evaluate whether the crystal represents a native conformation.

Determining the accessibility of membrane-permeable (Guan and Kaback, 2006; Guan and Kaback, 2007; Kozachkov et al., 2007; Nie et al., 2007; Tamura et al., 2001) and membrane-impermeable (Guan and Kaback, 2007; Karlin and Akabas, 1998; Tzubery, 2008) sulfhydryl reagents to cys-replacements has proved useful in tracing aqueous environments within or surrounding a membrane protein.

In line with the suggestion that the NhaA X-ray structure is native, the majority of the structural information obtained indirectly at physiological pH in the membrane when NhaA is active correlated well with the crystal structure obtained at pH 4 when NhaA is downregulated (Fig. 2) (Tzubery, 2008). Hence, the crystal structure of NhaA monomer is native, and many helices do not change conformation with pH.

The NhaA monomer is fully functional yet the dimer is crucial for the stability of the antiporter

In addition to cryo-EM of the 2-D crystals (Williams, 2000; Williams et al., 1999), biochemical and genetic experiments (Gerchman et al., 2001) and ESR (Hilger et al., 2005) studies have shown that NhaA is a dimer in the native membrane. As yet we do not have a 3-D crystal structure of the NhaA dimer. However, based on the NhaA crystal structure, the EM map and the distances measured by ESR and cross-linking, a high-resolution model of the NhaA dimer in the membrane was obtained (Fig. 3) (Hilger et al., 2007). The model shows that the dimer-interface is composed of the two β-hairpins of the two monomers, forming

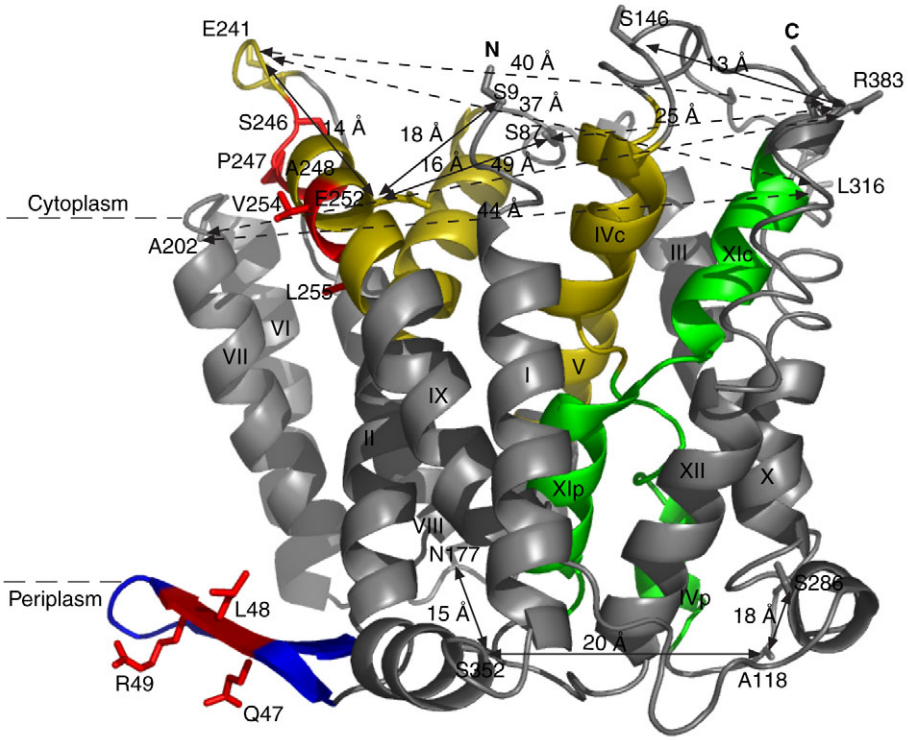

Fig. 2. Distances in the crystal structure are compared with those obtained by intra-molecular cross-linking. The overall architecture of NhaA is shown as in Fig. 1A. Transmembrane segments (TMSs) IVp and TMSs XI of the TMSs IV–XI assembly are marked green. Segments of the TMSs lining the cytoplasmic funnel (II, IVc, V and IX) are marked yellow. Residues in the NhaA dimer interface (in the β-sheet and the N-terminus of TMS IX) are marked red. Arrows and numbers denote distances between indicated amino acids residues. The membrane is depicted by the broken lines. The representation was generated using PyMOL software (http://pymol.sourceforge.net/).

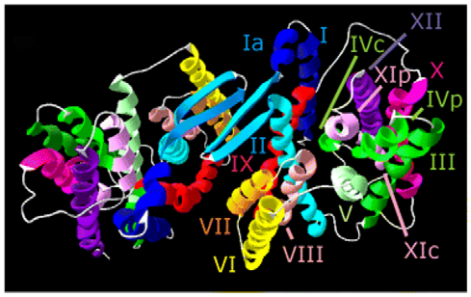

Fig. 3. Model structure of NhaA dimer based on ESR study. Overview of the NhaA dimer seen from the periplasmic side and shown in ribbon representation was reproduced, with permission, from Hilger and colleagues (Hilger et al., 2007).

an anti-parallel β-sheet at the periplasmic side of the molecule. Only a few amino acid residues in helix IX of one monomer and helix VII of the other monomer make contact with each other at the cytoplasmic face of the molecule. Intermolecular cross-linking experiments fully supported the suggested interface (Fig. 2) (Tzubery et al., 2008).

By constructing a NhaA mutant devoid of the β-hairpin (ΔP45–N58), we revealed that the β-hairpin is crucial for the dimeric state of NhaA (Rimon et al., 2007). On blue native polyacrylamide gel electrophoresis (BN-PAGE), the β-hairpin deletion (ΔP45–N58) has the mobility of a monomer, and it exists only as a monomer both in the native membrane and in β-DDM (*n*-dodecyl β-D-maltopyranoside) micelles. Furthermore, whereas the monomers cross-link in the membrane of the wild-type dimers, no cross-linking is observed with monomeric NhaA (Rimon et al., 2007).

Joint β-hairpins forming β-sheets are a classical motif of oligomer formation in soluble proteins (Maris et al., 2005; Rimon et al., 2007). Interestingly, the NhaA β-sheet is located parallel to the membrane in the periplasmic space outside the membrane (Fig. 1A; Fig. 2). Hence, we have revealed how an oligomerization motif of soluble proteins is recruited to form a dimer of a membrane protein (Padan, 2008).

Based on the NhaA crystal structure, it has been suggested that the monomer is the functional unit of NhaA (Hunte et al., 2005). In support of this suggestion, the monomeric NhaA mutant, with the β-hairpin deleted (ΔP45–AN58), is fully functional (Rimon et al., 2007). In isolated membrane vesicles and in reconstituted proteoliposomes, the Na^+/H^+ antiporter activity and pH regulation of the monomeric mutant was very similar to those of the wild-type dimer (Rimon et al., 2007). Notably, the NhaA dimer interface contains residues that are involved in the activity or regulation of the antiporter. Therefore, mutations of these residues and/or their cross-linking indirectly affect the antiporter activity and its regulation, with no direct relationship to the dimerization state (Rimon et al., 2007; Tzubery et al., 2008).

Although monomeric NhaA is functional, the dimer is beneficial under conditions of extreme stress. Under routinely used stress conditions (0.1 mol l^{-1} LiCl at pH 7 or 0.6 mol l^{-1} NaCl at pH 8.3), the monomeric NhaA confers salt resistance on NhaA- and NhaB-deleted cells as well as the wild type (Rimon et al., 2007). However, under conditions of extreme stress (0.1 mol l^{-1} LiCl or 0.7 mol l^{-1} NaCl both at pH 8.5), the advantage of the dimeric NhaA becomes apparent (Rimon et al., 2007). Whereas growth of the wild-type dimer was hardly affected, growth of the monomeric mutant was markedly reduced. Point mutations in the β-sheet (L48C, R49C) resulted in phenotypes similar to the mutation with the deletion (Herz et al., 2009).

We have recently found that both in β–DDM micelles and in the membrane, NhaA dimerization is crucial for the stability of the antiporter (Herz et al., 2009). We therefore suggest that the NhaA dimers are more suitable than the monomers to function under the most extreme stress conditions. Notably, many secondary transporters are oligomers (Padan, 2008; Veenhoff et al., 2002) and the reason for this is unknown in most cases. Future studies will reveal whether NhaA provides a clue.

The structural insights of the NhaA crystal structure

The fold of NhaA is novel because of the unique TMS IV/XI assembly (Fig. 1A; Fig. 4B; Fig. 5A) (Hunte et al., 2005). This assembly is composed of: (1) a pair of TMSs (IV and XI), oriented opposite each other in the membrane, i.e. inverted topology, TMS IV starts at the periplasmic face whereas TMS XI starts at the cytoplasmic face of the membrane. (2) Each of these TMSs is interrupted in the middle of the membrane by an extended chain. The partial-positive charges of the two opposing N-termini of TMS IV are charge-compensated and stabilized by D133 of extended chain IV (Fig. 5A). The partial-negative charges of the two opposing C-termini of TMS XI are compensated by K300 of helix X (Fig. 5A). Hence, the TMS IV/XI assembly is delicately balanced electrostatically, a property that is crucial for NhaA activity (Hunte et al., 2005; Padan, 2008).

Neither Na^+ nor Li^+ could be observed in the structure because of the medium resolution (Hunte et al., 2005). Nevertheless, based on solved structures of Na^+-binding sites (Boudker et al., 2007; Meier et al., 2005; Murata et al., 2003; Yamashita et al., 2005), we have suggested that the NhaA Na^+-binding site is at the extended chains of the TMS IV/XI assembly, very near the pit of the cytoplasmic funnel (Fig. 1B; Fig. 5A) (Hunte et al., 2005). The binding site includes the most conserved amino acid residues, D163, D164, D133 and T132. The first two residues are essential (Galili et al., 2002; Kuwabara et al., 2006). Replacement of the latter two residues dramatically increases the apparent K_M of the antiporter (Galili et al., 2004; Galili et al., 2002).

Most of the crystal structures of ion transporters that have been deciphered up to now show an intra-molecular inverted topology of several helices, including a pair of discontinuous helices, which are interrupted by an extended chain where the ion-binding site is located (Screpanti and Hunte, 2007). These include ATPases (Ca^{2+}-ATPase) (Fig. 4A) (Olesen et al., 2007; Takahashi et al., 2007; Toyoshima et al., 2000), Na^+/K^+-ATPase (Morth et al., 2007), the cytoplasmic membrane H^+-ATPase (Pedersen et al., 2007) and secondary transporters including NhaA (Fig. 4B) (Hunte et al., 2005), $LeuT_{Ae}$ (Fig. 4C) (Yamashita et al., 2005), ClC (Fig. 4D) (Dutzler et al., 2002), $GltT_{Ph}$ (Fig. 4E) (Yernool et al., 2004) and very recently, SGlT (Fig. 4F) (Faham et al., 2008).

The X-ray structures revealed that the extended chains, whose polar backbone groups are not fully saturated with internal hydrogen bonds, the partially charged helical termini and the polar or charged residues, in close proximity, provide the structural basis for the ion-binding site. The extended peptides create an open space, which accommodates a charged substrate in the otherwise densely packed α-helical integral membrane proteins. The presence of an ion is expected to perturb the delicate electrostatic compensation so that the ends of the helices can be exploited for substrate binding whereas the liberated residues compete with the

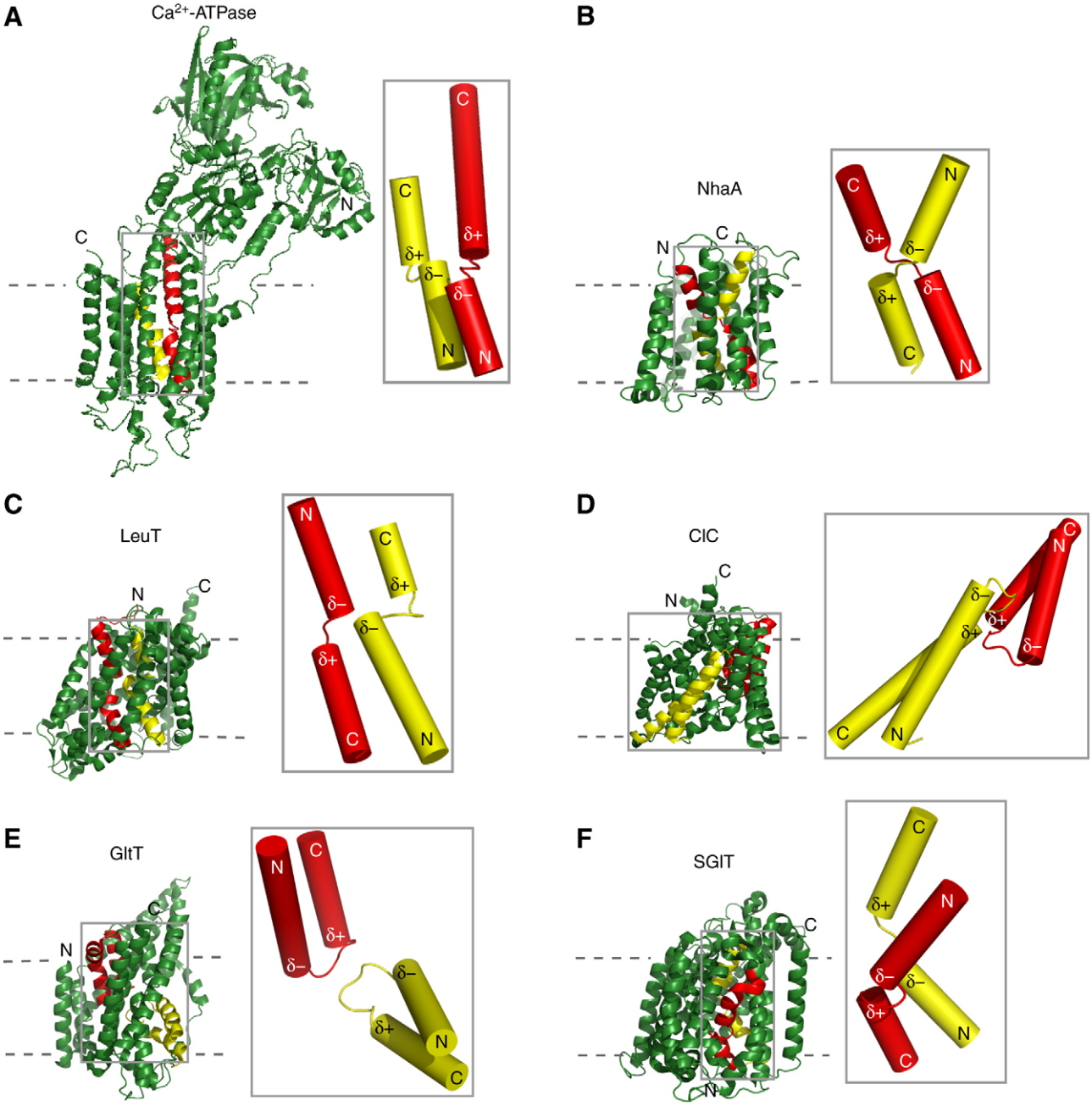

Fig. 4. Discontinuous membrane helices in transport proteins. Crystal structures of transport proteins with discontinuous helices. (A) Ca^{2+}-ATPase (Toyoshima et al., 2000). (B) NhaA (Hunte et al., 2005). (C) LeuT (Yamashita et al., 2005). (D) ClC (Dutzler et al., 2002). (E) GltT (Yernool et al., 2004). (F) SGlT (Faham et al., 2008). The left side of each panel shows the whole molecule (green) with the two discontinuous membrane helices colored in red and yellow according to their respective N- and C-termini. The right side of each panel shows an enlarged view of the discontinuous helices in cylindrical presentation. The partial charges at the termini are indicated. The estimated membrane position is shown (broken lines).

ion to avoid tight binding. Interestingly, in LeuT eukaryotic orthologs, free Cl^- or negatively charged residues on the transporter can provide charge-compensation for Na^+ transport (Forrest et al., 2007; Zomot et al., 2007). Relative to α-helices, extended chains may also confer flexibility at a lower energy cost and allow the conformational changes necessary for the alternate accessibility mechanism of ion transport. Recently, a molecular model of the alternate accessibility mechanism of transport has been advanced on the basis of the intra-molecular dual topology (Forrest et al., 2008).

The functional insights provided by the NhaA crystal structure

Genetic, biochemical and biophysical studies of NhaA have been used over the years to identify the location of the ion-binding site, the ‘pH sensor’ and the cation translocation and its regulation. Remarkably, projecting the experimental data onto the crystal structure has provided a static snapshot of the functional organization of NhaA (Fig. 5A).

A cluster of negatively charged residues at the orifice of the cytoplasmic funnel is most suited to attract cations and function as an ionic trap and, at the same time, serve as the ‘pH sensor’. Thus,

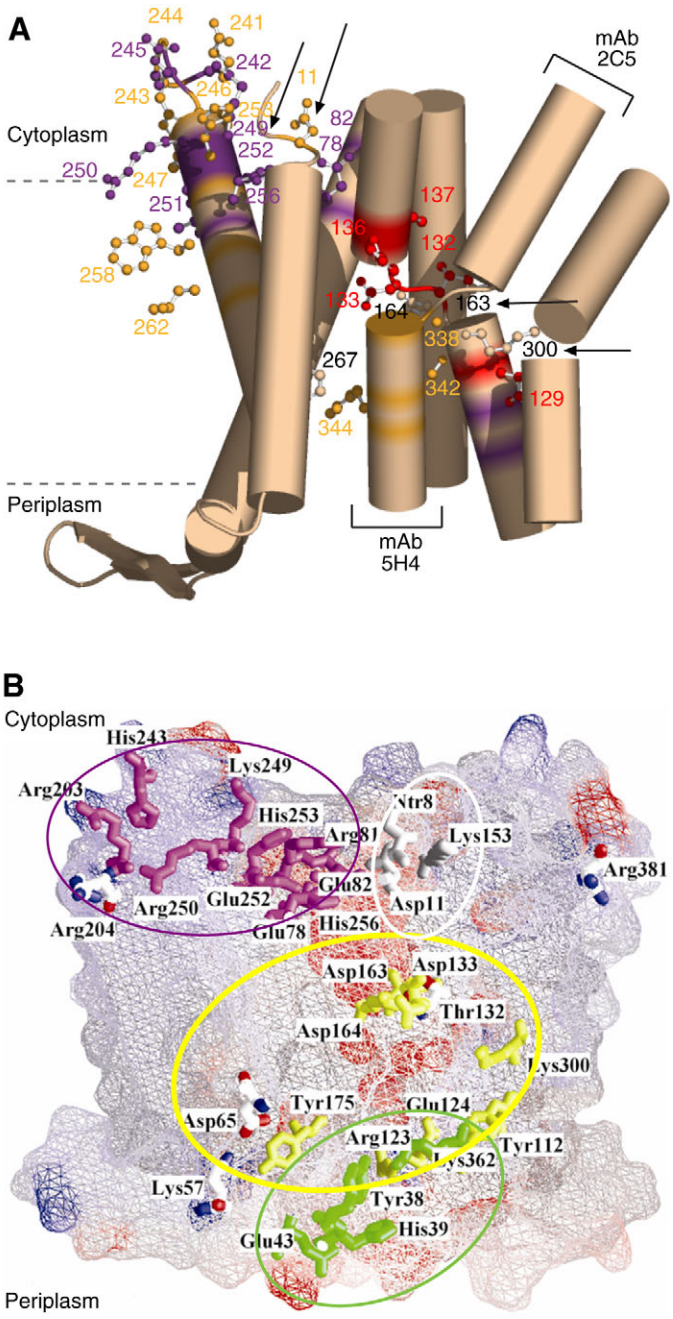

Fig. 5. Functional organization of NhaA Na^+/H^+ antiporter. (A) Cylindrical representation of functionally important NhaA transmembrane segments (TMSs) viewed parallel to the membrane (broken lines). A stick and ball representation of functionally important residues in the putative active site (red) and the 'pH sensor' (magenta) is shown. Residues in which cys-replacements affect only the pH-dependence of NhaA activity or both the pH-dependence and the apparent K_M for Na^+ are marked in yellow or magenta, respectively. The figure was prepared using PyMOL (http://pymol.sourceforge.net/). (B) Clusters of residues with strongly electrostatic interaction in NhaA as revealed *in silico* by multiconformation continuum electrostatics (MCCE) analysis (Olkhova et al., 2006). Four clusters of residues, which interact in a strong electrostatic manner cross NhaA along its cross-membrane axis: I, magenta; II, gray; III, yellow; IV, green. These are important for ion translocation and the 'pH sensor' of NhaA (see A). Zones of negative and positive potential are colored red and blue, respectively. For orientation, other residues are indicated in black. This figure was prepared after Olkhova et al. (Olkhova et al., 2006) using Grasp (Honig and Nicholls, 1995).

a 'pH signal' at the 'pH sensor' that alters the protonation state would elicit a conformational change, culminating in NhaA activation at the TMS IV/XI assembly.

To identify the amino acid residues that participate in the pH response, we conducted site-directed mutagenesis at amino acids whose p*K* values are in the physiological range (Galili et al., 2002; Gerchman et al., 1999; Kozachkov et al., 2007; Padan et al., 2004; Tzubery et al., 2008; Tzubery et al., 2003). Also carried out was random mutagenesis of plasmidic *nha*A, followed by a selection of mutants that affect the pH profile of cell growth (Rimon et al., 1998). Remarkably, the crystal structure has revealed that most of the mutations affecting the pH response cluster at the putative 'pH sensor', the N-terminus of TMS IX and at its target, the TMS XIp and the extended chains in the TMS IV/XI assembly range (Fig. 5A).

As described above, the ion-binding site is located at the pit of the cytoplasmic funnel (Fig. 1B; Fig. 5A) and is the site where the most conserved and essential residues in the NhaA family, D163 and D164, are located (Galili et al., 2004; Galili et al., 2002; Kuwabara et al., 2006). Only D164 is exposed to the funnel (Hunte et al., 2005) (Fig. 1B). Most probably, additional residues (D133 and T132), in the vicinity, participate in cation binding (Fig. 5A) (Galili et al., 2004; Galili et al., 2002).

The structure predicted the location of residues affecting the translocation in the TMS IV/XI assembly. To identify amino acid residues involved in NhaA ion translocation, we used the following approaches: (1) site-directed mutagenesis of amino acid residues that have the chemical capacity to attract, bind or repel cations (Galili et al., 2004; Galili et al., 2002); (2) mutagenesis of residues that in other proteins have been shown to bind Na^+ (Galili et al., 2002); and (3) random mutagenesis of plasmidic *nha*A and selected mutants that change the specificity or affinity to the ions (Galili et al., 2004; Galili et al., 2002). Remarkably, the mutations that affect the translocation cluster at the TMS IV/XI assembly (Fig. 5A).

The structure showed that helix IX, which harbors the 'pH sensor', is in direct contact with the TMSs IV/XI assembly *via* F267 and F344 (Fig. 5A). Remarkably, we have recently shown that cys-replacement of these residues affects the Na^+-H^+ stoichiometry of NhaA (Tzubery et al., 2008). Hence, by projecting available genetic, biochemical and biophysical data onto the 3-D crystal structure, we revealed that the 'pH sensor' at the orifice of the cytoplasmic funnel is separated by 15 Å from its target – the TMS IV/XI assembly (Fig. 5A).

The dynamics of NhaA

Like other secondary transporters, NhaA is a 'nano-machine' that converts one form of energy, the electrochemical gradient of H^+ ($\Delta\mu_{H^+}$), to another, the electrochemical gradient of Na^+ ($\Delta\mu_{Na^+}$), across the membrane. The downregulated NhaA crystal structure was obtained at pH 4. By comparison, NhaA activation occurs above pH 6 and is maximal at pH 8.5. Therefore, to enable us to understand the mechanism of NhaA activation and its pH regulation, the structures, functions and dynamics of all of the transitions must be identified. This task involves crystallizing all active conformations, a project that is currently in progress. In addition, structural information obtained by indirect methods as a function of a change in conditions (pH), can provide valuable information about transport dynamics (Guan and Kaback, 2006; Kozachkov et al., 2007; Nie et al., 2007; Tzubery et al., 2008; Zhou et al., 2008; Guan and Kaback, 2007). Moreover, the availability of crystal structures has opened up new research avenues, both *in situ* and *in silico*, which could not otherwise have been employed.

Structure-based computation unraveled the unique NhaA electrostatic organization (Olkhova et al., 2006). Using the multi-conformation continuum electrostatics (MCCE) method, we studied, *in silico*, the effect of pH values on the protonation state of ionisable residues in NhaA (Olkhova et al., 2006). The results have revealed that the NhaA electrostatic organization is unique (Fig. 5B); it contains four clusters of residues that are spread along the cross-membrane axis of the protein and interact in a strongly electrostatic manner. Cluster I, located at the N-terminal end of TMS IX at the orifice of the cytoplasmic funnel and Cluster II on the opposite side of the cytoplasmic funnel contain residues that form the 'pH sensor'. Cluster III, formed mainly by residues within the ion-binding site, including D163 and D164, is located at the middle of the membrane. Cluster IV is at the rim of the periplasmic funnel. H256 provides an electrostatic connection between Clusters I, II and III, and D133 connects Clusters I and III. We suggest that these unique electrostatic interactions between the clusters are essential for pH signal transduction across the membrane and NhaA activation (Olkhova et al., 2009).

Combining the MCCE studies with molecular dynamics (MD) simulations has revealed that a structural change must occur in few parts of NhaA whereas most helices do not change conformation (Fig. 2; Fig. 5B) (Olkhova et al., 2007). Remarkably, all predictions were validated experimentally (Fig. 5A). pH-induced conformational changes at the pH sensor were identified by a monoclonal antibody (Venturi et al., 2000) and by accessibility of NhaA to trypsin (Gerchman et al., 1999) or MIANS (Tzubery et al., 2003), which is a fluorescent probe. pH-induced movement of helix X toward helix II was verified by cross-linking (Kozachkov et al., 2007). pH-induced changes in the cytoplasmic funnel was demonstrated by testing the accessibility of Cys-replacements to various reagents of a size similar to hydrated Na^+ as a function of pH. It was validated that the cytoplasmic funnel is lined by helix IX and that the funnel deepens at physiological pH (Tzubery et al., 2008).

pH-induced movement in the TMS IV/XI assembly were not identified by cross-linking. This negative result can imply that there are no conformational changes at this location or that the experimental approach is not sensitive enough. Given the high turnover rate of NhaA (Taglicht et al., 1991), we prefer the latter alternative. Indeed, we could demonstrate that the TMS IV/XI assembly is most sensitive to conformational changes. Cross-linking of a dead double Cys-replacement mutant [T132C (TMS IV)-G338C (TMS XI)] revived the mutation thus highlighting the importance of the conformation at the TMS IV/XI assembly (Galili et al., 2004). Furthermore, epitopes of two conformational mAbs (2C5 and 5H4) that inhibit NhaA activity (Padan et al., 1998) have recently been mapped at both ends of TMS XI (Fig. 5A) (Rimon et al., 2008). Presumably, the mAbs exert torsion that change the conformation of the assembly and inhibit the antiporter.

Working hypothesis

As shown above, NhaA undergoes a reversible pH-induced conformational change(s) (Fig. 6A,B) by which NhaA is activated. At acidic pH, when NhaA is downregulated, only part of the cation-binding site (D164) is accessible to the cation passage whereas the periplasmic passage is blocked by the ion barrier. In response to a signal from the 'pH sensor', a conformational change in helix IX and X results in the reorientation of the active site. This exposes the full Na^+-Li^+ binding site (D164, D163 and most probably also D133 and T132) to the cytoplasmic passage and removes the periplasmic ion barrier, leaving the extended chain to seal off the binding site from the periplasm.

This conformation will now be ready for Na^+-H^+ exchange (Fig. 6B,C) in the alternate accessibility mechanism in which the transporter has two major alternating conformations, i.e. the substrate-binding site either facing inward or outward (Jencks, 1980). Inter-conversion between the two conformations in an antiporter is possible only *via* a substrate-bound form of the protein. We suggest that the TMS IV/XI assembly, with its interrupted helices and finely compensating dipoles in the middle of the

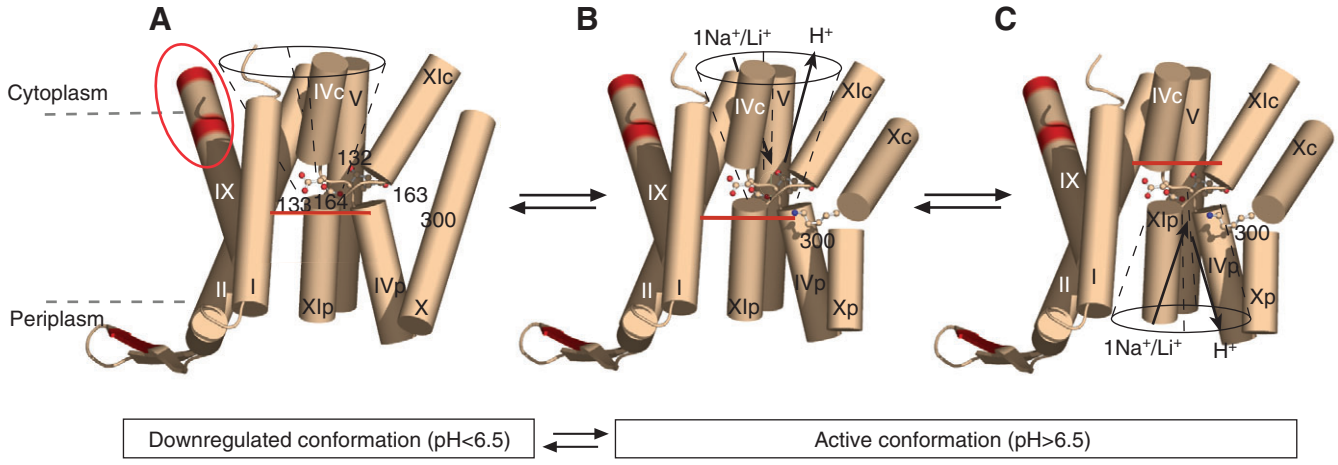

Fig. 6. Proposed mechanism of NhaA, a pH-regulated Na^+/H^+ antiporter. A schematic presentation of the pH-induced conformational changes (A,B) and the conformational changes accompanying Na^+ antiport (B,C) (A) Acidic pH-locked conformation. Ion translocation is prevented by the periplasmic ion barrier (transparent, orange colored zone and red bar) and by the only residue (D164) within the Na^+-Li^+-binding site (residues D164, D163, T132, D133) that is exposed to the cytoplasmic funnel (black dotted line and black circle). (B) Activation by alkaline pH induces conformational changes in the 'pH sensor' at the N-terminal of helix IX (red circle), resulting in reorientation of helices IVp, XIp and X. The putative Na^+-Li^+-binding site is now exposed to the cytoplasmic funnel but is sealed off towards the periplasm (red bar). (C) Na^+-Li^+ binding results in opening of the periplasmic funnel, which is sealed off from the cytoplasm (red bar) and exposure of the active site to the periplasm. The cation is released. Protonation of D163 and D164 brings the antiporter back to the active conformation, open to the cytoplasm. For orientation, the NhaA dimer interface is marked red at the N-terminus of helix IX and the β-sheet.

membrane, is best suited to the charge-induced subtle and rapid conformational changes needed for alternating access of the substrate-binding site to either the intracellular or the extracellular space. Na^+-Li^+ binding to the active site from the cytoplasm results in a charge imbalance that triggers small movements of XIc, XIp, IVc, IVp and their extended chains. As a result, the cation-loaded binding site will be exposed to the periplasm and sealed off from the cytoplasm. Upon Na^+-Li^+ release, both aspartates will become protonated thus inducing a conformational change that will re-expose them to the cytoplasm where deprotonation will complete the cycle. This model accommodates an overall stoichiometry of $2H^+/Na^+$or Li^+. Because NhaA activity is reversible, the magnitude of the electrochemical potential difference of Na^+-Li^+ relative to that of H^+ determines the direction of the cation exchange across the membrane. This mechanism differs from the mechanism postulated on the basis of the structure of five other secondary transporters, LacY (Abramson et al., 2003), ADP/ATP antiporter (Pebay-Peyroula et al., 2003), GlpT (Huang et al., 2003), AcrB (Murakami et al., 2006) and SGlT (Faham et al., 2008), in which heavily distorted helices line a wide substrate passage and a large part of the molecule assumes different conformations. This latter type of mechanism is suitable for these slowly turning over ($1000\,min^{-1}$) transporters of large organic molecules (Guan and Kaback, 2006; Nie et al., 2007). By contrast, NhaA is one of the fastest transporters as yet identified ($10{,}0000\,min^{-1}$). A model mechanism for Na^+-H^+ exchange has recently been suggested on the basis of MD (Arkin et al., 2007).

The crystal structure of NhaA provides insights into the human NHA1, NHA2 and NHE1

The crystal structure of NhaA has provided insights into the eukaryotic antiporter NHE1 and a unique human antiporter, which is expressed in the cytoplasmic membrane of every cell and serves as a house-keeping antiporter (Fliegel, 2008; Malo and Fliegel, 2006; Orlowski and Grinstein, 2007). It plays key roles in pathological conditions of the human heart and thus is a known target for drug design. Indeed, NHE1 inhibitors are used to relieve syndromes related to heart hypertrophy, ischemia and reperfusion. NHE1 differs from NhaA in three main characteristics: (1) it is an electroneutral antiporter exchanging 1 H^+ per 1 Na^+; (2) it uses the Na^+ gradient (directed inward) maintained by the Na^+-K^+-ATPase to excrete H^+ from the cytoplasm; and (3) it is tightly regulated by pH but in contrast to NhaA, it is activated at acidic pH. A thorough understanding of the structure–function relationship of NHE1 is, therefore, important for rational drug design and for understanding the mechanism of its antiport activity and specific regulation by pH.

Using the NhaA crystal structure as a template, and by employing bioinformatics and evolutionary approaches, we have predicted the 3-D structure of the membrane portion of human NHE1, which seems to be very similar to NhaA (Fig. 7A) (Landau et al., 2007). Modeling of this protein has been particularly challenging because of the extremely low sequence identity between these proteins (10–12%). Our model depicts 12 TMSs, with the C- and N-termini in the cytoplasm. As previously indicated, topology was based on hydrophobicity scales and accessibility of Cys-replacements to membrane-impermeant probes (Wakabayashi et al., 2000). Whereas the first TMS in our model begins at residue V129, Wakabayashi and colleagues have predicted two additional segments at the preceding N-terminal end (Wakabayashi et al., 2003). However, in agreement with our model, this segment is not required for functionality (Landau et al., 2007). Our structural model is supported by an evolutionary conservation analysis and empirical data. The model also reveals the location of the binding site of amiloride derivatives, NHE1 inhibitors. One of these, 2-aminoperimidine (2-AP) was shown to inhibit NhaA. The NHE1 model guided us in identifying the binding site of 2-AP on

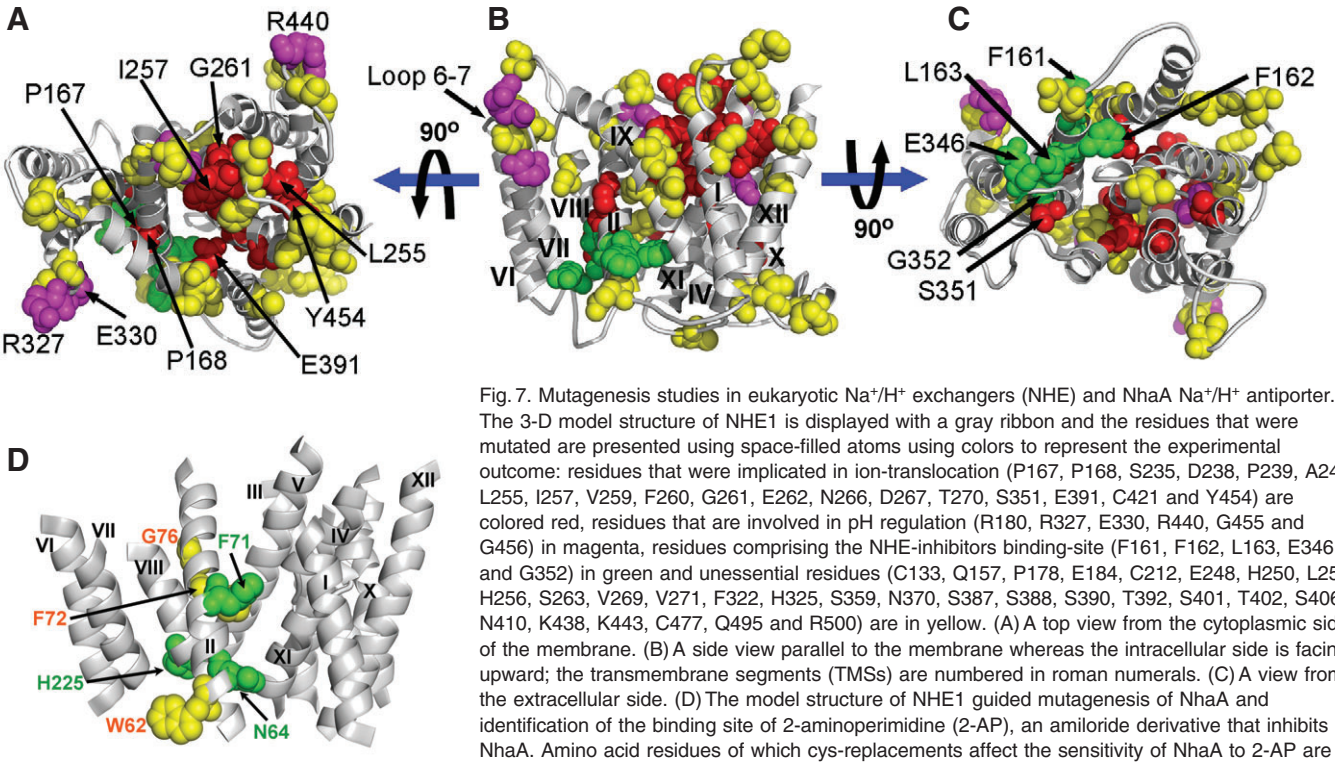

Fig. 7. Mutagenesis studies in eukaryotic Na^+/H^+ exchangers (NHE) and NhaA Na^+/H^+ antiporter. The 3-D model structure of NHE1 is displayed with a gray ribbon and the residues that were mutated are presented using space-filled atoms using colors to represent the experimental outcome: residues that were implicated in ion-translocation (P167, P168, S235, D238, P239, A244, L255, I257, V259, F260, G261, E262, N266, D267, T270, S351, E391, C421 and Y454) are colored red, residues that are involved in pH regulation (R180, R327, E330, R440, G455 and G456) in magenta, residues comprising the NHE-inhibitors binding-site (F161, F162, L163, E346 and G352) in green and unessential residues (C133, Q157, P178, E184, C212, E248, H250, L254, H256, S263, V269, V271, F322, H325, S359, N370, S387, S388, S390, T392, S401, T402, S406, N410, K438, K443, C477, Q495 and R500) are in yellow. (A) A top view from the cytoplasmic side of the membrane. (B) A side view parallel to the membrane whereas the intracellular side is facing upward; the transmembrane segments (TMSs) are numbered in roman numerals. (C) A view from the extracellular side. (D) The model structure of NHE1 guided mutagenesis of NhaA and identification of the binding site of 2-aminoperimidine (2-AP), an amiloride derivative that inhibits NhaA. Amino acid residues of which cys-replacements affect the sensitivity of NhaA to 2-AP are marked green. Naïve residues are marked yellow.

NhaA by mutagenesis (Fig. 7D) (Landau et al., 2007). The NHE1 model structure features a cluster of titratable residues that are evolutionarily conserved and located in a conserved region in the center of the membrane, in a pattern similar to that of NhaA (Fig. 7A–C). We suggest that these residues are involved in cation binding and translocation and that the structural fold of the antiporter is evolutionary conserved.

NhaA orthologs have recently been discovered in eukaryotes (Brett et al., 2005). Phylogenetic analysis has shown that NHAs are found in all phyla for which genomes are available. They have been found expressed in many eukaryotic tissues with most interesting functional implications. The human NHA2 has been suggested to be a candidate gene for human essential hypertension (Xiang et al., 2007). The tissue localization of *Ag*NHA1 (*Anopheles gambiae* NHA1) suggests that it functions with the V-ATPase to maintain the characteristic longitudinal pH gradient in the lumen of the alimentary canal of the larvae (Okech et al., 2008; Rheault et al., 2007; Wieczorek et al., 2009). Co-localization with the V-ATPase was also found in Drosophila (Day et al., 2008). NHA2 has been assigned a role in osteoclasts development in the mouse (Battaglino et al., 2008). Another intriguing suggestion is that NHA2 is localized at the mitochondrial membrane (Battaglino et al., 2008; Fuster et al., 2008) and is possibly responsible for the mitochondrial NhaA activity revealed by Mitchell and Moyle more than 40 years ago (Mitchell and Moyle, 1965).

In contrast to *Ec*NhaA, of which the protein has been purified and the crystal structure has been determined and the properties and pH-regulation have been most extensively studied (present review; Padan, 2008), no eukaryotic NHA has been purified. Therefore, the NHA properties are as yet not known, and the NHAs functional characterization has been based on their tissue and sub-cellular localization and expression and their capacity to rescue Na^+-Li^+-sensitive yeast mutants, which lack essential antiporters (Day et al., 2008; Fuster et al., 2008; Maresova and Sychrova, 2006; Xiang et al., 2007). *In vivo* evidence that *Ag*NHA1 is electrogenic is presented in this issue (Harvey, 2009); a voltage-dependent inward current and Na^+-dependent cell acidification in *Ag*NHA1-transfected *Xenopus* oocytes. Based on the crystal structure of *E. coli* NhaA, we are currently constructing a model of the human NHA2 (M. Xiang, M. Shushan, E.P., R. Rao and N. Bental, unpublished results). This model will be of great help in directing mutagenesis for the study of structure–function relationship of the NHA antiporters.

Conclusions

The determination of the NhaA crystal structure (Hunte et al., 2005) has provided insights into the mechanism of NhaA and its unique mode of pH-dependent regulation that might not otherwise have been uncovered. The monomer is the functional unit of NhaA yet the NhaA dimer is important for the stability of the antiporter (Rimon et al., 2007). A snapshot of the functional organization of NhaA has been elucidated whereby amino acid residues that form the 'pH sensor' (Galili et al., 2004; Galili et al., 2002; Tzubery et al., 2008; Tzubery et al., 2003) cluster at the orifice of the cytoplasmic funnel and are clearly separated (by 15 Å) from the cation active site located at the middle of the TMS IV/XI assembly; a new fold that is composed of helices interrupted by extended chains (Hunte et al., 2005). This assembly is delicately balanced electrostatically, a property that is likely to be crucial for NhaA activity (Padan, 2008). Importantly, helices interrupted by extended chains have recently been found to be common in ion binding and in the translocation of ion-transport proteins (Padan, 2008). New avenues of structural-based research have been opened up both *in silico* and *in situ*, and the unique electrostatic organization of NhaA and its role in the pH-dependent activity has been revealed (Olkhova et al., 2006; Olkhova et al., 2007). pH-induced conformational changes have been identified in NhaA (Gerchman et al., 1999; Kozachkov et al., 2007; Rimon et al., 2008; Tzubery et al., 2003; Venturi et al., 2000). A structural model of the human NHE1 has been built (Landau et al., 2007), representing an important step towards structure-based drug design. Combining structure-based methods with the determination of the crystal structures of NhaA active conformations should help to answer many general and NhaA-specific questions, i.e. what are the roles of the interrupted helices and the oligomeric states of ion transport proteins? How antiporter proteins function and how are they regulated by pH?

Research in the laboratory of E.P. is supported by a grant from the United States–Israel Binational Science Foundation (501/03-16.2) and EDICT (EU FP 7, European Drug Initiative on Channels and Transporters).

References

Abramson, J., Smirnova, I., Kasho, V., Verner, G., Kaback, H. R. and Iwata, S. (2003). Structure and mechanism of the lactose permease of *Escherichia coli*. *Science* **301**, 610-615.

Apse, M. P. and Blumwald, E. (2007). Na^+ transport in plants. *FEBS Lett.* **581**, 2247-2254.

Arkin, I. T., Xu, H., Jensen, M. O., Arbely, E., Bennett, E. R., Bowers, K. J., Chow, E., Dror, R. O., Eastwood, M. P. and Flitman-Tene, R. (2007). Mechanism of Na^+/H^+ antiporting. *Science* **317**, 799-803.

Battaglino, R. A., Pham, L., Morse, L. R., Vokes, M., Sharma, A., Odgren, P. R., Yang, M., Sasaki, H. and Stashenko, P. (2008). NHA-oc/NHA2: a mitochondrial cation-proton antiporter selectively expressed in osteoclasts. *Bone* **42**, 180-192.

Baumeister, W. and Steven, A. C. (2000). Macromolecular electron microscopy in the era of structural genomics. *Trends Biochem. Sci.* **25**, 624-631.

Boudker, O., Ryan, R. M., Yernool, D., Shimamoto, K. and Gouaux, E. (2007). Coupling substrate and ion binding to extracellular gate of a sodium-dependent aspartate transporter. *Nature* **445**, 387-393.

Brett, C. L., Donowitz, M. and Rao, R. (2005). Evolutionary origins of eukaryotic sodium/proton exchangers. *Am. J. Physiol. Cell Physiol.* **288**, 223-239.

Day, J. p., Wan, S., Allen, A. K., Kean, L., Davies, S. A., Gray, J. V. and Dow, J. A. T. (2008). Identification of two partners from the bacterial Kef exchanger family for the apical plasma membrane V-ATPase of metazoa. *J. Cell Sci.* **121**, 2612-2619.

Dutzler, R., Campbell, E. B., Cadene, M., Chait, B. T. and MacKinnon, R. (2002). X-ray structure of a ClC chloride channel at 3.0 Å reveals the molecular basis of anion selectivity. *Nature* **415**, 287-294.

Faham, S., Watanabe, A., Besserer, G. M., Cascio, D., Specht, A., Hirayama, B. A., Wright, E. M. and Abramson, J. (2008). The crystal structure of a sodium galactose transporter reveals mechanistic insights into Na^+/sugar symport. *Science* **321**, 810-814.

Fliegel, L. (2008). Molecular biology of the myocardial Na^+/H^+ exchanger. *J. Mol. Cell Cardiol.* **44**, 228-237.

Forrest, L. R., Tavoulari, S., Zhang, Y. W., Rudnick, G. and Honig, B. (2007). Identification of a chloride ion binding site in Na^+/Cl -dependent transporters. *Proc. Natl. Acad. Sci. USA* **104**, 12761-12766.

Forrest, L. R., Zhang, Y. W., Jacobs, M. T., Gesmonde, J., Xie, L., Honig, B. H. and Rudnick, G. (2008). Mechanism for alternating access in neurotransmitter transporters. *Proc. Natl. Acad. Sci. USA* **105**, 10338-10343.

Fuster, D. G., Zhang, J., Shi, M., Bobulescu, I. A., Andersson, S. and Moe, O. W. (2008). Characterization of the sodium/hydrogen exchanger NHA2. *J. Am. Soc. Nephrol.* **19**, 1547-1556.

Galili, L., Rothman, A., Kozachkov, L., Rimon, A. and Padan, E. (2002). Trans membrane domain IV is involved in ion transport activity and pH regulation of the NhaA-Na^+/H^+ antiporter of *Escherichia coli*. *Biochemistry* **41**, 609-617.

Galili, L., Herz, K., Dym, O. and Padan, E. (2004). Unraveling functional and structural interactions between transmembrane domains IV and XI of NhaA Na^+/H^+ antiporter of *Escherichia coli*. *J. Biol. Chem.* **279**, 23104-23113.

Gerchman, Y., Rimon, A. and Padan, E. (1999). A pH-dependent conformational change of NhaA Na^+/H^+ antiporter of *Escherichia coli* involves loop VIII-IX, plays a role in the pH response of the protein, and is maintained by the pure protein in dodecyl maltoside. *J. Biol. Chem.* **274**, 24617-24624.

Gerchman, Y., Rimon, A., Venturi, M. and Padan, E. (2001). Oligomerization of NhaA, the Na^+/H^+ antiporter of *Escherichia coli* in the membrane and its functional and structural consequences. *Biochemistry* **40**, 3403-3412.

Guan, L. and Kaback, H. R. (2006). Lessons from lactose permease. *Annu. Rev. Biophys. Biomol. Struct.* **35**, 67-91.

Guan, L. and Kaback, H. R. (2007). Site-directed alkylation of cysteine to test solvent accessibility of membrane proteins. *Nat. Protoc.* **2**, 2012-2017.

Harvey, W. R. (2009). Voltage coupling of primary H^+ V-ATPases to secondary Na^+- or K^+-dependent transporters. *J. Exp. Biol.* **212**, 1620-1629.

Herz, K., Vimont, S., Padan, E. and Berche, P. (2003). Roles of NhaA, NhaB, and NhaD Na^+/H^+ antiporters in survival of *Vibrio cholerae* in a saline environment. *J. Bacteriol.* **185**, 1236-1244.

Herz, K., Rimon, A., Jeschke G. and Padan, E. (2009). β-Sheet-dependent dimerization is essential for the stability of NhaA Na^+-H^+ antiporter. *J. Biol. Chem.* **284**, 6337-6347.
Hilger, D., Jung, H., Padan, E., Wegener, C., Vogel, K. P., Steinhoff, H. J. and Jeschke, G. (2005). Assessing oligomerization of membrane proteins by four-pulse DEER: pH-dependent dimerization of NhaA Na^+/H^+ antiporter of *E. coli*. *Biophys J.* **89**, 1328-1338.
Hilger, D., Polyhach, Y., Padan, E., Jung, H. and Jeschke, G. (2007). High-resolution structure of a Na^+/H^+ antiporter dimer obtained by pulsed EPR distance measurements. *Biophys. J.* **93**, 3675-3683.
Honig, B. and Nicholls, A. (1995). Classical electrostatics in biology and chemistry. *Science* **268**, 1144-1149.
Huang, Y., Lemieux, M. J., Song, J., Auer, M. and Wang, D. N. (2003). Structure and mechanism of the glycerol-3-phosphate transporter from *Escherichia coli*. *Science* **301**, 616-620.
Hunte, C., Screpanti, M., Venturi, M., Rimon, A., Padan, E. and Michel, H. (2005). Structure of a Na^+/H^+ antiporter and insights into mechanism of action and regulation by pH. *Nature* **534**, 1197-1202.
Jencks, W. P. (1980). The utilization of binding energy in coupled vectorial processes. *Adv. Enzymol. Relat. Areas Mol. Biol.* **51**, 75-106.
Karlin, A. and Akabas, M. H. (1998). Substituted-cysteine accessibility method. *Methods Enzymol.* **293**, 123-145.
Kozachkov, L., Herz, K. and Padan, E. (2007). Functional and structural interactions of the transmembrane domain X of NhaA, Na^+/H^+ antiporter of *Escherichia coli*, at physiological pH. *Biochemistry* **46**, 2419-2430.
Kuwabara, N., Inoue, H., Tsuboi, Y., Mitsui, K., Matsushita, M. and Kanazawa, H. (2006). Structure-function relationship of the fifth transmembrane domain in the Na^+/H^+ antiporter of *Helicobacter pylori*: topology and function of the residues, including two consecutive essential aspartate residues. *Biochemistry* **45**, 14834-14842.
Landau, M., Herz, K., Padan, E. and Ben-Tal, N. (2007). Model structure of the Na^+/H^+ exchanger 1 (NHE1): functional and clinical implications. *J. Biol. Chem.* **282**, 37854-37863.
Malo, M. E. and Fliegel, L. (2006). Physiological role and regulation of the Na^+/H^+ exchanger. *Can. J. Physiol. Pharmacol.* **84**, 1081-1095.
Maresova, L. and Sychrova, H. (2006). *Arabidopsis thaliana* CHX17 gene complements the kha ! deletion phenotypes in *Sacharomyces cerevisiae*. *Yeast* **23**, 1167-1171.
Maris, A. E., Walthers, D., Mattison, K., Byers, N. and Kenney, L. J. (2005). The response regulator OmpR oligomerizes *via* beta-sheets to form head-to-head dimers. *J. Mol. Biol.* **350**, 843-856.
Meier, T., Polzer, P., Diederichs, K., Welte, W. and Dimroth, P. (2005). Structure of the rotor ring of F-Type Na^+-ATPase from *Ilyobacter tartaricus*. *Science* **308**, 659-662.
Mitchell, P. and Moyle, J. (1965). Stoichiometry of proton translocation through the respiratory chain and adenosine triphospatase system of rat liver mitochondria. *Nature* **208**, 147-151.
Morth, J. P., Pedersen, B. P., Toustrup-Jensen, M. S., Sorensen, T. L., Petersen, J., Andersen, J. P., Vilsen, B. and Nissen, P. (2007). Crystal structure of the sodium-potassium pump. *Nature* **450**, 1043-1049.
Murakami, S., Nakashima, R., Yamashita, E., Matsumoto, T. and Yamaguchi, A. (2006). Crystal structures of a multidrug transporter reveal a functionally rotating mechanism. *Nature* **443**, 173-179.
Murata, T., Arechaga, I., Fearnley, I. M., Kakinuma, Y., Yamato, I. and Walker, J. E. (2003). The membrane domain of the Na^+-motive V-ATPase from *Enterococcus hirae* contains a heptameric rotor. *J. Biol. Chem.* **278**, 21162-21167.
Nie, Y., Ermolova, N. and Kaback, H. R. (2007). Site-directed alkylation of LacY: effect of the proton electrochemical gradient. *J. Mol. Biol.* **374**, 356-364.
Okech, B. A., Boudko, D. Y., Linser, P. J. and R. H. W. (2008). Cationic pathway of pH regulation in larvae of *Anopheles gambiae*. *J. Exp. Biol.* **211**, 957-968.
Olami, Y., Rimon, A., Gerchman, Y., Rothman, A. and Padan, E. (1997). Histidine 225, a residue of the NhaA-Na^+/H^+ antiporter of *Escherichia coli* is exposed and faces the cell exterior. *J. Biol. Chem.* **272**, 1761-1768.
Olesen, C., Picard, M., Winther, A. M., Gyrup, C., Morth, J. P., Oxvig, C., Moller, J. V. and Nissen, P. (2007). The structural basis of calcium transport by the calcium pump. *Nature* **450**, 1036-1042.
Olkhova, E., Hunte, C., Screpanti, E., Padan, E. and Michel, H. (2006). Multiconformation continuum electrostatics analysis of the NhaA Na^+/H^+ antiporter of *Escherichia coli* with functional implications. *Proc. Natl. Acad. Sci. USA* **103**, 2629-2634.
Olkhova, E., Padan, E. and Michel, H. (2007). The influence of protonation states on the dynamics of the NhaA antiporter from *Escherichia coli*. *Biophysics J.* **92**, 3784-3791.
Olkhova, E., Kozachkov, L., Padan E. and Michel, H. (2009). Combined computational and biochemical study reveals the importance of electrostatic interactions between the 'pH sensor' and the cation binding site of the sodium/proton antiporter NhaA of *Escherichia coli*. *Proteins* (in press).
Orlowski, J. and Grinstein, S. (2004). Diversity of the mammalian sodium/proton exchanger SLC9 gene family. *Pflugers Arch.* **447**, 549-565.
Orlowski, J. and Grinstein, S. (2007). Emerging roles of alkali cation/proton exchangers in organellar homeostasis. *Curr. Opin. Cell Biol.* **19**, 483-492.
Padan, E. (2008). The enlightening encounter between structure and function in the NhaA-Na^+/H^+ antiporter. *Trends Biochem. Sci.* **33**, 435-443.
Padan, E., Zilberstein, D. and Rottenberg, H. (1976). The proton electrochemical gradient in *Escherichia coli* cells. *Eur. J. Biochem.* **63**, 533-541.
Padan, E., Venturi, M., Michel, H. and Hunte, C. (1998). Production and characterization of monoclonal antibodies directed against native epitopes of NhaA, the Na^+/H^+ antiporter of *Escherichia coli*. *FEBS Lett.* **441**, 53-58.
Padan, E., Venturi, M., Gerchman, Y. and Dover, N. (2001). Na^+/H^+ antiporters. *Biochim. Biophys. Acta* **1505**, 144-157.
Padan, E., Tzubery, T., Herz, K., Kozachkov, L., Rimon, A. and Galili, L. (2004). NhaA of *Escherichia coli*, as a model of a pH-regulated Na^+/H^+ antiporter. *Biochim. Biophys. Acta* **1658**, 2-13.
Padan, E., Bibi, E., Masahiro, I. and Krulwich, T. A. (2005). Alkaline pH homeostasis in bacteria: new insights. *Biochim. Biophys. Acta* **1717**, 67-88.
Pebay-Peyroula, E., Dahout-Gonzalez, C., Kahn, R., Trezeguet, V., Lauquin, G. J. and Brandolin, G. (2003). Structure of mitochondrial ADP/ATP carrier in complex with carboxyatractyloside. *Nature* **426**, 39-44.
Pedersen, B. P., Buch-Pedersen, M. J., Morth, J. P., Palmgren, M. G. and Nissen, P. (2007). Crystal structure of the plasma membrane proton pump. *Nature* **450**, 1111-1114.
Pham, L., Purcell, p., Morse, L. R., Stashenko, P. and Battaglino, R. A. (2007). Expression analysis of *nha-oc*/NHA2: A novel gene selectively expressed in osteoclasts. *Gene Expr. Patterns* **7**, 846-851.
Rheault, M. R., Okech, B. A., Keen, S. B. W., Miller, M. M. and Harvey, W. R. (2007). Molecular cloning, physiology and localization of AgNHA1: the first Na^+/H^+ antiporter (NHA) from a metazoan, *Anopheles gambiae*. *J. Exb. Biol.* **210**, 3848-3861.
Rimon, A., Gerchman, Y., Kariv, Z. and Padan, E. (1998). A point mutation (G338S) and its suppressor mutations affect both the pH response of the NhaA-Na^+/H^+ antiporter as well as the growth phenotype of *Escherichia coli*. *J. Biol. Chem.* **273**, 26470-26476.
Rimon, A., Tzubery, T., Galili, L. and Padan, E. (2002). Proximity of cytoplasmic and periplasmic loops in NhaA Na^+/H^+ antiporter of *Escherichia coli* as determined by site-directed thiol cross-linking. *Biochemistry* **41**, 14897-14905.
Rimon, A., Tzubery, T. and Padan, E. (2007). Monomers of NhaA Na^+/H^+ antiporter of *Escherichia coli* are fully functional yet dimers are beneficial under extreme stress conditions at alkaline pH in the presence of Na^+ or Li^+. *J. Biol. Chem.* **282**, 26810-26821.
Rimon, A., Hunte, C., Michel, H. and Padan, E. (2008). Epitope mapping of conformational monoclonal antibodies specific to NhaA Na^+/H^+ antiporter: structural and functional implications. *J. Mol. Biol.* **379**, 471-481.
Screpanti, E. and Hunte, C. (2007). Discontinuous membrane helices in transport proteins and their correlation with function. *J. Struct. Biol.* **159**, 261-267.
Screpanti, E., Padan, E., Rimon, A., Michel, H. and Hunte, C. (2006). Crucial steps in the structure determination of the Na^+/H^+ antiporter NhaA in its native conformation. *J. Mol. Biol.* **362**, 192-202.
Slepkov, E. R., Rainey, J. K., Sykes, B. D. and Fliegel, L. (2007). Structural and functional analysis of the Na^+/H^+ exchanger. *Biochem J.* **401**, 623-633.
Taglicht, D., Padan, E. and Schuldiner, S. (1991). Overproduction and purification of a functional Na^+/H^+ antiporter coded by *nhaA* (*ant*) from *Escherichia coli*. *J. Biol. Chem.* **266**, 11289-11294.
Taglicht, D., Padan, E. and Schuldiner, S. (1993). Proton-sodium stoichiometry of NhaA, an electrogenic antiporter from *Escherichia coli*. *J. Biol. Chem.* **268**, 5382-5387.
Takahashi, M., Kondou, Y. and Toyoshima, C. (2007). Interdomain communication in calcium pump as revealed in the crystal structures with transmembrane inhibitors. *Proc. Natl. Acad. Sci. USA* **104**, 5800-5805.
Tamura, N., Konishi, S., Iwaki, S., Kimura-Someya, T., Nada, S. and Yamaguchi, A. (2001). Complete cysteine-scanning mutagenesis and site-directed chemical modification of the Tn10-encoded metal-tetracycline/H^+ antiporter. *J. Biol. Chem.* **276**, 20330-20339.
Toyoshima, C., Nakasako, M., Nomura, H. and Ogawa, H. (2000). Crystal structure of the calcium pump of sarcoplasmic reticulum at 2.6 Å resolution. *Nature* **405**, 647-655.
Tzubery, T. (2008). The relationship between structure, pH sensing and pH regulation of NhaA-Na^+/H^+ antiporter of *Escherichia coli* In *Institute of Life Sciences*, pp. 118. PhD thesis, Hebrew University, Jerusalem.
Tzubery, T., Rimon, A. and Padan, E. (2003). Mutation E252C increases drastically the Km value for Na^+ and causes an alkaline shift of the pH dependence of NhaA Na^+/H^+ antiporter of *Escherichia coli*. *J. Biol. Chem.* **279**, 3265-3272.
Tzubery, T., Rimon, A. and Padan, E. (2008). Structure-based functional study reveals multiple roles of TMS IX and loop VIII-IX in NhaA Na^+/H^+ antiporter of *Escherichia coli* at physiological pH. *J. Biol. Chem.* **283**, 15975-15987.
Veenhoff, L. M., Heuberger, E. H. and Poolman, B. (2002). Quaternary structure and function of transport proteins. *Trends Biochem. Sci.* **27**, 242-249.
Venturi, M. and Padan, E. (2002). Purification of NhaA Na^+/H^+ antiporter of *Escherichia coli* for 3D and 2D crystallization. In *A Practical Guide to Membrane Protein Purification* (ed. C. Hunte, G. Von Jagow and H. Schagger), pp. 179-190. Amsterdam: Elsevier.
Venturi, M., Rimon, A., Gerchman, Y., Hunte, C., Padan, E. and Michel, H. (2000). The monoclonal antibody 1F6 identifies a pH-dependent conformational change in the hydrophilic NH_2 terminus of NhaA Na^+/H^+ antiporter of *Escherichia coli*. *J. Biol. Chem.* **275**, 4734-4742.
Wakabayashi, S., Pang, T., Su, X. and Shigekawa, M. (2000). A novel topology model of the human Na(+)/H(+) exchanger isoform 1. *J. Biol. Chem.* **275**, 7942-7949.
Wakabayashi, S., Pang, T., Hisamitsu, T. and Shigekawa, M. (2003). *The sodium-Hydrogen Exchange, from Molecule to its Role in Disease*. Boston, MA: Kluwer.
Wieczorek, H., Beyenbach, K. W., Huss, M. and Vitavska, O. (2009). Vacuolar-type proton pumps in insect epithelia. *J. Exp. Biol.* **212**, 1611-1619.
West, I. C. and Mitchell, P. (1974). Proton/sodium ion antiport in *Escherichia coli*. *Biochem. J.* **144**, 87-90.
Williams, K. A. (2000). Three-dimensional structure of the ion-coupled transport protein NhaA. *Nature* **403**, 112-115.
Williams, K. A., Geldmacher-Kaufer, U., Padan, E., Schuldiner, S. and Kuhlbrandt, W. (1999). Projection structure of NhaA, a secondary transporter from *Escherichia coli*, at 4.0 Å resolution. *EMBO J.* **18**, 3558-3563.

Xiang, M., Feng, M., Muend, S. and Rao, R. (2007). A human Na^+/H^+ antiporter sharing evolutionary origins with bacterial NhaA may be a candidate gene for essential hypertension. *Proc. Natl. Acad. Sci. USA* **104**, 18677-18681.
Yamaguchi, T. and Blumwald, E. (2005). Developing salt-tolerant crop plants: challenges and opportunities. *Trends Plant Sci.* **10**, 615-620.
Yamashita, A., Singh, S. K., Kawate, T., Jin, Y. and Gouaux, E. (2005). Crystal structure of a bacterial homologue of Na^+/Cl^--dependent neurotransmitter transporters. *Nature* **437**, 215-223.
Yernool, D., Boudker, O., Jin, Y. and Gouaux, E. (2004). Structure of a glutamate transporter homologue from *Pyrococcus horikoshii*. *Nature* **431**, 811-818.
Zhou, Y., Guan, L., Freltes, J. and Kaback, H. (2008). Opening and closing of the periplasmic gate in lactose permease. *Proc. Natl. Acad. Sci. USA* **105**, 3774-3778.
Zomot, E., Bendahan, A., Quick, M., Zhao, Y., Javitch, J. A. and Kanner, B. I. (2007). Mechanism of chloride interaction with neurotransmitter:v sodium symporters. *Nature* **449**, 726-730.